Pak. j. sci. ind. res. Ser. A: phys. sci. 2025 **68A**(2) 186-192

Symmetric Surface State for TM Polarised Mode at Air Semiconductor Photonic Hypercrystal Interface

Hasnain Haider and Munazza Zulfiqar Ali
University of the Punjab, Physics Department, Quaid-i-Azam Campus, Lahore-54590, Pakistan

(received June 12, 2023; revised May 29, 2024; accepted May 30, 2024)

Abstract. It is theoretically examined whether electromagnetic surface waves manifest at the interface between air and photonic hypercrystals for the transverse magnetic polarisation mode (TM). Photonic hypercrystals are created by arranging HMMs into periodic photonic crystal. It is found that the studied surface waves have modest losses and are symmetric with respect to the positive and negative directions of surface propagation. The relationship between these waves and the hyperbolic metamaterial layers filling factor and the crystal itself is developed by curve graphing.

Keywords: photonic crystal, metamaterial, hyperbolic metamaterial, photonic hypercrystal, surface waves, surface plasmon-polaritons

Introduction

The unique phenomenon of photonic hypercrystals is the result of the integration of the two seemingly unrelated domains of photonic crystals and metamaterials (Galfsky *et al*., 2017; Galfsky *et al*., 2016; Huang and Narimanov, 2014a and 2014b; Smolyaninova *et al*., 2014). The bandwidth and light emission properties of photonic crystals and metamaterials are both constrained, but when they are coupled to form photonic hypercrystals, these properties may improve. Periodic structures include photonic crystals (PCs) with bands and gaps enabling light propagation in an optical medium (Sakoda, 2001). Their capacity to regulate the flow of light on a very small length scale has garnered a lot of interest (Akahane *et al*., 2003). Lord Rayleigh (Rayleigh, 2009) and Sajeev John (John, 1987) produced two important research on PC by establishing that these systems display a one-dimensional photonic band-gap. Yablonovitch had previously developed the first three dimensional photonic band gap in the microwave range (Yablonovitch *et al*.,1987). Materials with characteristics not seen in naturally occurring materials are referred to as metamaterials (Baron *et al*., 2020). A metamaterial is an engineered composite that possesses superior properties not found in nature or in constituent materials, according to the definition given. Negative refractive index metamaterials (NIMs) are materials that simultaneously exhibit negative permittivity and permeability and negative refraction (Foteinopoulou *et al*., 2003). A number of fascinating features have been postulated, realized and shown in lab settings, including, EM black holes, superlensing (Pendry, 2000) and invisibility cloaking (Schurig *et al*., 2006). In the meantime, engineering has also produced useful tools and antennas. The "hyperbolic metamaterials" (HMMs) nomenclature is derived from the topology of the iso-frequency surface. The linear dispersion and isotropic behaviour of propagating waves in vacuum imply a spherical iso-frequency surface. HMMs are one of the areas of modern optics that are evolving the quickest (Noginov *et al*., 2013; Guo *et al*., 2012) with a single axis. A tensor having two distinct components that represent the directions along (ετ) and across (εn) Uniaxial crystals dielectric properties are described in terms of the interface. $(\varepsilon_n) > 0$, $(\varepsilon_\tau) < 0$, $(\varepsilon_\tau) > 0$, $(\varepsilon_n) > 0$, (ε_τ) . $(\varepsilon_n) < 0$ respectively, denote a dielectric medium, a metal, or a hyperbolic metamaterial. The equal frequency surface of exceptional (transverse magnetic polarised) waves, which corresponds to a one- or two-sheet hyperbola in k-space depending on the permittivity tensor signature, is the source of the HMMs' unique features. Quantum nanophotonics (Jacob, 2012; Jacob and Narimanov, 2008) Dyakonov plasmonics nanoimaging, subsurface sensing (Guo *et al*., 2012), super-Planckian thermal, fluorescence engineering and emission control (Jacob *et al*., 2012) will all be important areas of application (Jacob and Shalaev, 2011). The amplitude of the wave vector k in HMMs is nearly infinite, and the local density of photonic states is also nearly infinite (Huang and Narimanov, 2014a). By inserting a periodic variation with a period that is higher than the period of the HMM ($\Lambda >> d_H$) but lower than the free space

*Author for correspondence; E-mail: ha7nain@gmail.com

wavelen ($\Lambda << \lambda_0$), a PHC (Narimanov, 2014) is created. The required periodic variation can be achieved by inserting a second media, which could be a metal, a dielectric, or a hyperbolic medium with a distinct dielectric permittivity tensor, in the composition's design. Dirac physics and singularities (Narimanov, 2015), which are extensively employed in macroscopic optical systems like resonators (Hafezi *et al*., 2013) are applicable to PHC properties (Ali, 2021), such as a larger spontaneous emission rate and bandwidth enhancement compared to PC and HMMs. Self-assembly has lately enabled the realisation of passive structures as PHC (Smolyaninova *et al*., 2014) and magnetic hyperbolic dispersion in optical frequencies has also been achieved. Dispersion relations and wave propagation in PHC have been studied via theoretical research work in 2017 (Ali, 2017) and dispersion relation for the TM polarized nonlinear surface waves in photonic hypercrystals has been derived and founded that the nonlinearity can be used to engineer the group velocity of the resulting surface wave. Recentaly the dispersion properties of the surface waves decaying in red-shifted and blue-shifted gaps in photonic hypercrystals are studied (Haider and Ali, 2023).

Mathematical formalism. Surface TM-polarized wave propagation in the air-PHC interface, This consists of periodic dielectric layers with permittivity (ε_d), a uniaxial hyperbolic medium with permittivity tensor (ε_H) and air, with corresponding thickness d_d, d_H and d_a, respectively.

HMMs are now the most promising artificial media for use in the visible and near-infrared wavelength bands (Shamonina and Solymar, 2007). In order to approximate the multilayer structure of HMMs as homogenous anisotropic material, the effective medium theory can be used. A multilayer composite is a uniaxial anisotropic multilayer structure (Podolskiy and Narimanov, 2005) with effective medium permittivities composed of alternating metallic and dielectric layers. The layers are in the xy plane and the z-axis is perpendicular to them. The permittivities of the metallic and dielectric layers, (ε_m) and (ε_d) and the associated layer widths are given as d_d and d_m.

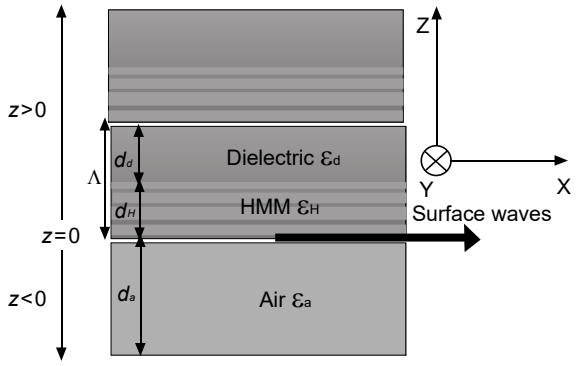

Fig. 1. An illustration of dielectric hyperbolic media with air at its surface, the photonic hyper crystal is terminated with air.

The method uses a generalised Maxwell-garnett methodology to produce analytical formulations for the effective permittivity in the parallel (ε_τ) and perpendicular (ε_n) directions specified for the multilayer hyperbolic metamaterial. The following definitions can be used to determine the filling factor (P) of the system's total metal thickness to the system's total thickness of the hyperbolic metamaterial and the dispersion relation:

$$\varepsilon_\tau = P\varepsilon_m + (1 - P)\varepsilon_d \quad \text{..... (1)}$$

$$\varepsilon_n = \frac{1}{\frac{P}{\varepsilon_m} + \frac{(1 - P)}{\varepsilon_d}} \quad \text{..... (2)}$$

$$\frac{w^2}{c^2} = \frac{k^2x}{\varepsilon_\tau} + \frac{k^2z}{\varepsilon_n} \quad \text{..... (3)}$$

The TE and TM dispersion relation gives wave vectors for metalic,hyperbolic and dielectric medium as:

$$k_m = \sqrt{\varepsilon_m k_0^2 - k_\tau^2} \quad \text{..... (4)}$$

$$k_H = \sqrt{\varepsilon_\tau k_0^2 - \left(\frac{\varepsilon_\tau}{\varepsilon_n}\right) k_\tau^2} \quad \text{..... (5)}$$

$$k_d = \sqrt{\varepsilon_d k_0^2 - k_\tau^2} \quad \text{..... (6)}$$

Principal dielectric constants ($\varepsilon_x = \varepsilon_y \neq \varepsilon_z$) are not identical in hyperbolic medium. Consequently, there are two types of anisotropic media, each of which is distinguished by having a distinct sign for the primary dielectric constant. Type 1: ($\varepsilon_n > 0$, $\varepsilon_\tau < 0$) and Type 2: ($\varepsilon_\tau < 0$, $\varepsilon_n > 0$) are shown in Fig. 2.

Surface wave is a mechanical wave that moves along the boundary between two media, according to its

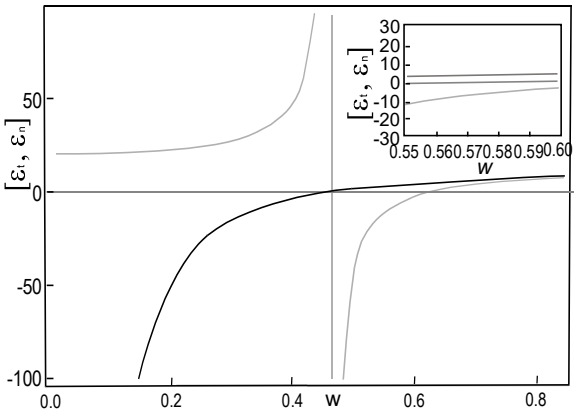

Fig. 2. Plot of ε_τ (blue) and ε_n (green) *vs* frequency and W indicating type II hyperbolic metamaterial at frequencies less than W=0.5, the value of $\varepsilon_\tau, < 0$, $\varepsilon_n > 0$ and type I $\varepsilon_\tau > 0$, $\varepsilon_n < 0$ hyperbolic metamaterial at frequencies within W>0.5 and W0.6, respectively.

definition. In the same way, they can be directed at an interface between two mediums with various dielectric constants, electromagnetic waves can also propagate as "surface waves" (Lax and Nelson, 1976).

Let an isotropic, homogeneous substance with a relative permittivity scalar of ε_a an occupy half-space for $z \leq 0$. According to Fig. 1, the 1D PHC with period Λ occupies the region $Z \geq 0$. Roughly coupled wave analysis (RCWA) is a semi-analytical method employed in computational electromagnetics to analyze scattering in periodic dielectric structure (Polo *et al*., 2013). With respect to x, the reflected as well as transmitted field phasors can be expressed as Fourier series for the region filled by either partnered material, so the photonic crystal's period is given by $\Lambda = d_1 + d_2$.

The x-axis in the XY plane is assumed to be the direction of surface wave propagation in the field phasors for TM modes (Ali, 2018), For all $z \in (-\infty, \infty)$ where q is the surface wave's complex wavenumber along the direction of propagation.

$$\underline{E}(\underline{r}) = \{e_x(z)\,\underline{u}_x + e_z(z)\underline{u}_z\}e^{iqx} \quad \text{..... (4)}$$

$$\underline{H}(\underline{r}) = \{h_y(z)\,\underline{u}_y\}e^{iqx} \quad \text{..... (5)}$$

One ordinary differential equation and two algebraic equations produced when the aforementioned equations are substituted into the Maxwell equations for the electric and magnetic field phasors.

$$\frac{d}{d_x} e_x(z) - iqe_z(z) = iwu_o e_y(z)$$

$$\frac{d}{d_z} h_y(z) - = iw\varepsilon_n\varepsilon_o d_x(z)$$

$$qhy(z) = -w\varepsilon_\tau\varepsilon_o e_x(z)$$

Equations' sums can have an endless number of terms. In addition, there are an endless number of equations. It is impossible to use this endless set of equations in real life. Truncating the series yields an approximation, just like with any other Fourier series. By removing $e_z(z)$ and $h_z(z)$, the matrix ordinary differential equation was obtained. The P-polarization states' equations. The matrix differential equation is satisfied by the field phasors.

$$\frac{d}{d_z}\begin{bmatrix} e_x(z) \\ n_o\, h_y(z) \end{bmatrix} = i\begin{bmatrix} 0 & n_o\left(w\mu_o - \dfrac{q^2}{w\varepsilon_\tau\varepsilon_o}\right) \\ n_o\,(w\varepsilon_n\varepsilon_o) & 0 \end{bmatrix}$$

$$\begin{bmatrix} e_x(z) \\ n_o\, h_y(z) \end{bmatrix} \quad \text{..... (6)}$$

P-Polarization state defined as $[f^{(p)}(z)] = [e_x(z)\, n_o\, h_y(z)]^T$ and using $n_o = \sqrt{\frac{\mu_o}{\varepsilon_o}}$, $w = \frac{k_o}{\sqrt{\mu_o\varepsilon_o}}$ and $ko = w\sqrt{\mu_o\varepsilon_o}$ in differential equation the analytical solution for $z \in (0, \Lambda)$ to yield.

$$[f^{(p)}(\Lambda)] = \begin{bmatrix} Q^{(p)} \\ \Lambda^{(q,z)} \end{bmatrix}[f^{(p)}(0, +)] \quad \text{..... (7)}$$

For PHC we can write as:

$$\left[Q^{(p)}_{PHC}\right] = \left[W^{(p)}_{HMM}\right]\left[W^{(p)}_{d}\right]$$

A matrix can be defined as follows *via* the Floquet-Lyapunov theorem:

$$\left[Q^{(p)}_{PHC}\right] = \exp\left\{i\Lambda Q^{(p)}_{PHC}\right\} \quad \text{..... (8)}$$

$$\left[W^{(p)}_{HMM}\right] = \exp\left[i2\pi W\begin{bmatrix} 0 \\ \varepsilon_\perp\left(1 - \dfrac{q^2}{k_0^2\varepsilon_d}\right) \\ 0 \end{bmatrix} D_1\right] \quad \text{..... (9)}$$

$$\left[W_d^{(p)}\right] = \exp\left[i2\pi W \begin{bmatrix} 0 \\ \varepsilon_d\left(1 - \frac{q^2}{k_0^2\varepsilon_d}\right) \\ 0 \end{bmatrix} D_2\right] \quad \text{..... (10)}$$

After multiplication of (9) and (10) we get:

$$\left[Q_{PHC}^{(p)}\right] = \begin{bmatrix} X_{11} & X_{12} \\ X_{21} & X_{22} \end{bmatrix} \quad \text{..... (11)}$$

Let $\left[V_{PHC}^{(p)}\right]$, be the Eigen vector associated with $\left[Q_{PHC}^{(p)}\right]$ nth Eigen value g. The field phasors must be written using the Eigen vectors corresponding to the Eigen values Im[g] > 0 in order to guarantee that the surface waves decay with $Z \to \infty$.

$$\left[f^{(p)}(0\ +)\right] = \left[V_{PHC}^{(p)}\right] B_\Lambda^{(p)}$$

$$\left[V_{PHC}^{(p)}\right] = \begin{bmatrix} - \frac{X_{12}}{X_{11} - g} \end{bmatrix} \quad \text{..... (12)}$$

where:

$B_\Lambda^{(p)}$ unknown dimensionless scalars and g are is Eigen value of the Eigen vector $\left[V_{PHC}^{(p)}\right]$.

Additionally, surface waves' electromagnetic fields must decay as z. $\to \infty$. Assuming $[V_a^{(p)}$, n ε [1,2], represent the Eigen vectors for nth Eigen value *a* of $\left[Q_{PHC}^{(p)}\right]$. Therefore, in the half space $z \to -\infty$, the Eigen vectors corresponding to the Eigen values Im[*a*] < 0 must be used to write the field phasors.

$$\left[f^{(p)}(0\ -)\right] = \left[V_a^{(p)}\right] B_a^{(p)}$$

$$[Va] = \begin{bmatrix} \sqrt{\varepsilon_\alpha - Q^2} \\ \varepsilon_\alpha \\ 1 \end{bmatrix} \quad \text{..... (13)}$$

where:

$B_a^{(p)}$ are unknown dimensionless scalars.

Therefore, $\left[f^{(p)}(0\ -)\right] = \left[f^{(p)}(0\ +)\right]$, which may be rewritten as the matric equation, is necessary for the uniformity of the electric and magnetic field phasors' tangential components across the z=0 plane.

$$\left[Y^{(p)}\right] \begin{bmatrix} B_\Lambda^{(p)} \\ B_\alpha^{(p)} \end{bmatrix} = \begin{bmatrix} 0 \\ 0 \end{bmatrix} \quad \text{..... (14)}$$

For the dispersion relation, $\left[Y^{(p)}\right] = -\left[V_{PHC}^{(p)}\right]\left[V_a^{(p)}\right]$ and for nontrivial solutions, the 2 × 2 matrices $\left[Y^{(p)}\right]$, so that $\left[Y^{(p)}\right] = 0$.

$$\frac{X_{12}}{X_{11}{}^{-g}} = \frac{\sqrt{\varepsilon_a - Q^2}}{\varepsilon_a} = 0 \quad \text{..... (15)}$$

This is the surface waves dispersion equation. For the linear wave propagation, the dielectric material's electric permittivity, ε_d, is regarded as constant. A computational programme was created using the Mathematica programme to calculate the dispersion relation using the newton raphson method, it made it possible for PHC to direct both the real and imaginary portions of wave number Q of the numerous SPP waves. To address the TM modes of surface wave propagation.

Results and Discussions

For photonic hyper crystal (Narimanov *et al*., 2014), we take a HMMs super lattice based on doped semi-conductor. Dielectric layer is 250 nm wide consisting of $A_{l0.48}In_{0.52}As$ and HMMS based on $In_{0.53}Ga_{0.47}As_{0.48}$, here a superlattice with a thickness of 250 nm is used to separate the "dielectric" and "metallic" components of these HMMs in the mid-IR frequency region. $In_{0.53}Ga_{0.47}As$ act like a metal and $Al_{0.48}In_{0.52}As$ act as a dielectric substance. For the computational work, d_H = 250nm, d_d = 250nm, ε_d = 10.23, ε_α = 1, we are taking plasma wavelength as $\lambda_p = 5\mu m$ thus $w_p = \frac{2\pi c}{\lambda_p} = 377 \times 10^{12}$Hz. Width and frequency are de-dimensional as $D_1 = \frac{d_H}{\Lambda} = 0.5$, $D_2 = \frac{d_d}{\Lambda} = 0.5$, $W = \frac{\Lambda}{\lambda_0}$, $\Lambda = d_H + d_d = 500$nm, $Wp = \frac{w_p \Lambda}{c} = 0.6283$, $\varepsilon_m = 12.15$ $\left(1 - \frac{w_p^2}{W^2}\right)$ and $Q = \frac{q^2}{k_0}$.

Here, $P = {}^{P} = \frac{d_m}{d_m + d_d} = 0.5$ is the hyperbolic metamaterial layer filling factor, Here we have considered a finite periodic structure consisting of two periods. Where d_m are d_d are the widths of the metallic and dielectric layers in the hyperbolic metamaterial, respectively. To create a photonic hypercrystal, the width of this dielectric substance is periodically altered. The dielectric layer's width is D2, while the hyperbolic metamaterial layer's width is D1. Although we can use this method to define

the effective permittivity of the entire structure as $\lambda >> \Lambda$ being the period of the photonic hypercrystal, we won't be able to observe gaps in the frequency and wave vector regimes. Therefore, the entire structure is treated moving forward as a periodic structure made up of alternate layers of HMM (with permittivity tensor $\varepsilon_H = \begin{bmatrix} \varepsilon_\tau & 0 & 0 \\ 0 & \varepsilon_\tau & 0 \\ 0 & 0 & \varepsilon_n \end{bmatrix}$ and dielectric material (with permittivity ε_d). Here we have considered a finite periodic structure consisting of two periods.

The dispersion curves for the surface wave that match to equation (15) are shown in Fig. 3a and 3b for various ratios of layer thickness. The dispersion for materials including length elements is explained by curve "A" as D1 = 0.4, D2 = 0.6, similarly for "B" D1 = 0.5 and D2 = 0.5, for "C" D1 = 0.6 and D2 = 0.4 and for "D" D1 = 0.7 and D2 = 0.3, while the filling factor remain same. It is seen that by increasing the ratio of HMMs in the PHC, the surface waves shift higher in frequency, also these waves are deep sub wavelength as $Q = \frac{q}{k_0} > 1$ and propagate in both negative and positive direction along the x-axis as the curve A and B for positive and negative q are quite symmetric. Because it cannot be resolved on the scale of -0.5 to 0.05 illustrated above in Fig. 3c, it is important to note that the imaginary part of the wave vector for these surface waves is zero.

Similar to this, the surface wave dispersion curves shown in Fig. 4 are plotted for various filling factor values with P1 = 0.30, P2 = 0.40, P3 = 0.45 and P4 = 0.50, while the ratio of layer thickness of hyperbolic and dielectric medium remains same which is D1 = 0.5 and D2 = 0.5. It has been seen by increasing the filling factor of HMMs in PHC the surface wave's shifts higher in frequency likewise Fig 3a and also these waves are too deep sub wavelength and their propagation is along x-axis.

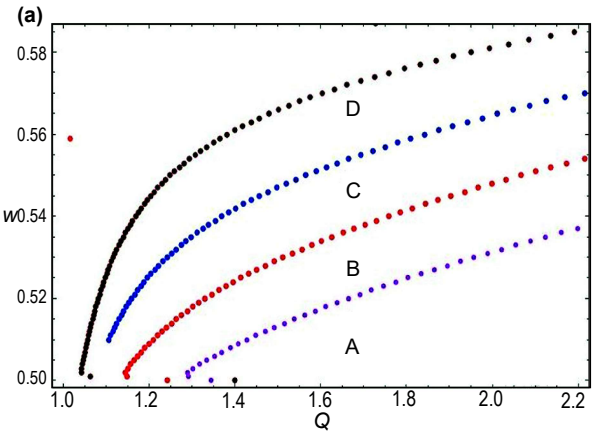

Fig. 3a. Plot of wave vector Q *vs* frequency W (de-dimensionlised parameters) for positive real values where filling factor is constant.

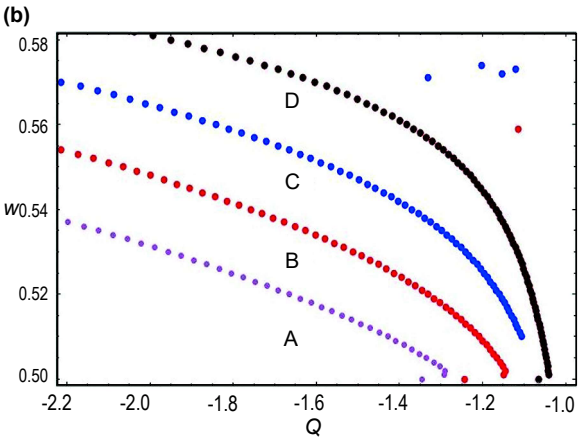

Fig. 3b. The graph of wave vector Q vs frequency W (de-dimensionlised parameters) for negative real values where filling factor is constant.

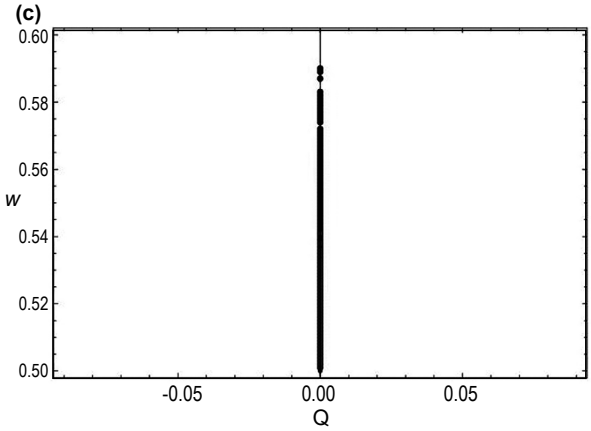

Fig. 3c. The graph of wave vector Q vs frequency W (de-dimensionlised parameters) for positive and negative Imaginary values where filling factor is constant.

Conclusion

In conclusion, this study looks at the linear surface waves in photonic hyper crystals. In photonic hyper crystals, dispersion relation for linear SPP waves with TM polarization is derived. SPP wave propagation can

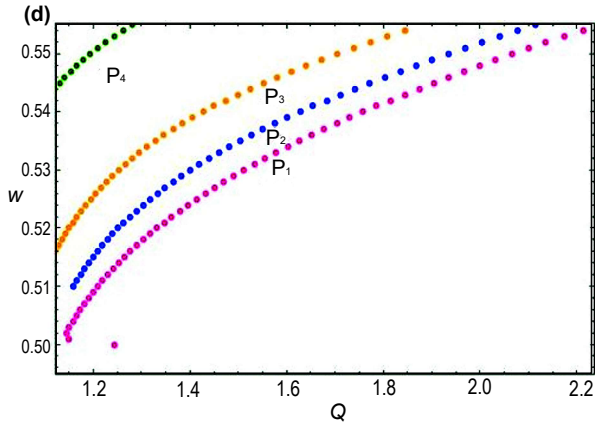

Fig. 4. The graph of wave vector Q *vs* frequency W (de-dimensionlised parameters) for Different value of P where D1 = 0.5 and D2 = 0.5.

also be examined when anisotropic material and a photonic hyper crystal are combined and this will provide more information. The infinite divergence of the surface wave vectors is likewise restricted by the non linearity. It is Envisaged that this preliminary study would serve as a foundation for future research on photonic hyper crystals, which will take into account nonlinear wave propagation in these structures under various approximations. It is found that nonlinearity can be used to manipulate the group velocity of the resulting surface wave.

Conflict of Interest. The authors declare that they have no conflict of interest.

References

Akahane, Y., Asano, T., Song, B.S., Noda, S. 2003. High-Q photonic nano cavity in a two dimensional photonic crystal. *Nature Letter*, **425:** 944-947.

Ali, M.Z. 2021. Plasmon-polariton gap and associated phenomenon of optical bistability in photonic hypercrystals. *Physics Letter A*, **387:** 127026-5.

Ali, M.Z. 2018. Dispersion relations and wave propagation in photonic hyper crystals. *Modern Physics Letter B*, **32:** 1750320-7.

Ali, M.Z. 2017. Nonlinear surface waves in photonic hypercrystals. *Physics Letter A*, **381:** 2643-2647.

Baron, A., Aradian, A., Ponsinet, V., Barois, P. 2020. Bottom-up nano-colloidal meta-materials and meta-surfaces at optical frequencies. *Comptes Rendus Physique*, **21:** 443-465.

Foteinopoulou, S., Economou, E.N., Soukoulis, C.M. 2003. Refraction in media with a negative refractive index. *Physical Review Letters*, **90:** 107402-4.

Galfsky, T., Gu, J., Narimanov E.E., Menon, V.M. 2017. Photonic hypercrystals for control of light-matter interactions. In: *Proceedings of the National Academy of Sciences*, **114:** 5125-5129.

Galfsky, T., Sun, Z., Considine, C.R., Chou, C.T., Ko, W.C., Lee, Y.H., Narimanov, E.E., Menon, V.M. 2016. Broadband enhancement of spontaneous emission in two-dimensional semiconductors using photonic hypercrystals. *Nano Letter*, **16:** 4940-4945.

Guo, T., Cortes, C.L., Molesky, S., Jacob, Z. 2012. Broadband super-Planckian thermal emission from hyperbolic metamaterials. *Applied Physics Letter*, **101:** 131106-5.

Guo, Y., Newman, W., Cortes, C.L., Jacob, Z. 2012. Applications of hyperbolic meta-material substrates. *Advances in Opto Electronics*, **452502:** 1-9.

Hafezi, M., Mittal, S., Fan, J., Migdall, A., Taylor, J.M. 2013. Imaging topological edge states in silicon photonics. *Nature Photonics*, **7:** 1001-1005.

Haider, H., Ali, M.Z. 2023. Dispersion properties of surface waves decaying in red-shifted and blue-shifted gaps in photonic hypercrystals. *Advanced in Condensed Matter Physcis*, **6773192:** 1-8.

Huang, Z., Narimanov, E.E. 2014a. Veselago lens by photonic hyper crystals. *Applied Physics Letter*, **105:** 031101-5.

Huang, Z., Narimanov, E.E. 2014b. Optical imaging by photonic hypercrystal: Veselago lens and beyond. *Journal of Optics*, **16:** 114009-7.

Jacob, Z., Shalaev, V.M. 2011. Plasmonics goes quantum. *Science*, **334:** 463-464.

Jacob, Z. 2012. Quantum Plasmonics. *MRS Bulletin*, **37:** 761-767.

Jacob, Z., Narimanov, E.E. 2008. Optical hyperspace for Plasmon's: Dyakonov states in metamaterials. *Applied Physics Lett*er, **93:** 221109-3.

Jacob, Z., Smolyaninov, I.I., Narimanov, E.E. 2012. Broadband purcell effect: radioactive decay engineering with metamaterials. *Applied Physics Letter*, **100:** 181105-4.

John, S. 1987. Strong localization of photons in certain disordered dielectric super lattices. *Physical Review Letter*, **58:** 2486-2489.

Lax, M., Nelson, D.F. 1976. Maxwell equations in material form. *Physical Review B*, **13:** 1777-1784.

Narimanov, E.E. 2015. Dirac dispersion in photonic

hyper crystals. *Faraday Discussions*, **178:** 45-59.

Narimanov, E.E. 2014. Photonic hypercrystals. *Physical Review X*, **4:** 041014-13.

Noginov, M., Lapine, M., Podolskiy, V., Kivshar, Y. 2013. Focus issue: hyperbolic meta-materials. *Optics Express*, **21:** 14895-14897.

Pendry, J.B. 2000. Negative refraction makes a perfect lens. *Physical Review Letter*, **85:** 3966-3969.

Polo, J., Mackay, T., Lakhtakia, A. 2013. *Electromagnetic Surface Waves: a Modern Perspective*. Elsevier, Amsterdam, Netherlands. https://doi.org/10.1016/C2011-0-07510-5

Podolskiy, V.A., Narimanov, E.E. 2005. Strongly anisotropic waveguide as a nonmagnetic left-handed system. *Physical Review B*, **71:** 201101-4.

Sakoda, K. 2001. Optical properties of photonic crystals. *Springer Series in Optical Science*, **80:** 99-123. https://doi.org/10.1007/978-3-662-14324-7_5

Schurig, D., Mock, J.J., Justice, B.J., Cummer, S.A., Pendry, J.B., Starr, A.F., Smith, D.R. 2006. Metamaterial electromagnetic cloak at microwave frequencies. *Science*, **314:** 977-980.

Shamonina, E., Solymar, L. 2007. Metamaterials: how the subject started. *Metamaterials*, **1:** 12-18.

Smolyaninova, V.N., Yost, B., Lahneman, D., Narimanov, E.E., Smolyaninov, I.I. 2014. Self-assembled tunable photonic hypercrystals. *Scientific Reports*, **4:** 5706-9.

Rayleigh, L. 2009. XXVI. On the remarkable phenomenon of crystalline reflation described by prof. Stokes. *The London, Edinburgh, and Dublin Philosophical Magazine and Journal of Science*, **26:** 256-265.

Yablonovitch, E., Gmitter, T.J., Meade, R.D., Rappe, A.M., Brommer, K.D., Joannopoulos, J.D. 1987. Inhibited spontaneous emission in solid-state physics and electrons. *Physical Review Letter*, **58:** 2059-2062.